ESC European Society of Cardiology

European Heart Journal (2021) **42**, 4481–4492
doi:10.1093/eurheartj/ehab412

Glucosylceramide synthase deficiency in the heart compromises β1-adrenergic receptor trafficking

Linda Andersson[1], Mathieu Cinato [1], Ismena Mardani[1], Azra Miljanovic[1], Muhammad Arif [2], Ara Koh [1,3], Malin Lindbom[1], Marion Laudette[1], Entela Bollano [1], Elmir Omerovic [1], Martina Klevstig[1], Marcus Henricsson [1], Per Fogelstrand[1], Karl Swärd[4], Matias Ekstrand [1], Max Levin [1], Johannes Wikström[5], Stephen Doran [6], Tuulia Hyötyläinen [7], Lisanna Sinisalu[7], Matej Orešič [8,9], Åsa Tivesten [1], Martin Adiels [1], Martin O. Bergo [10], Richard Proia [11], Adil Mardinoglu[2,6], Anders Jeppsson [1], Jan Borén[1], and Malin C. Levin[1]*

[1]Department of Molecular and Clinical Medicine/Wallenberg Laboratory, Institute of Medicine, the Sahlgrenska Academy at University of Gothenburg and Sahlgrenska University Hospital, Bruna Stråket 16, SE-413 45 Gothenburg, Sweden; [2]Science for Life Laboratory, KTH—Royal Institute of Technology, Stockholm, Sweden; [3]Department of Precision Medicine, School of Medicine, Sungkyunkwan University (SKKU), Suwon 16419, Republic of Korea; [4]Department of Experimental Medical Science, Lund University, SE-221 84 Lund, Sweden; [5]Bioscience, Research and Early Development, Cardiovascular, Renal and Metabolism, BioPharmaceuticals R&D, AstraZeneca, Gothenburg, Pepparedsleden 1, SE-431 83 Mölndal, Sweden; [6]Centre for Host-Microbiome Interactions, Faculty of Dentistry, Oral & Craniofacial Sciences, King's College London, London SE1 9RT, UK; [7]School of Natural Sciences and Technology, Örebro University, Fakultetsgatan 1, SE-701 82 Örebro, Sweden; [8]School of Medical Sciences, Örebro University, SE-701 82 Örebro, Sweden; [9]Turku Bioscience Centre, University of Turku, FIN-20521 Turku, Finland; [10]Department of Biosciences and Nutrition, Karolinska Institute, SE-141 83 Huddinge, Sweden; and [11]National Institute of Diabetes and Digestive and Kidney Diseases (NIDDK), National Institutes of Health, Bethesda, MD 20892, USA

Received 12 November 2020; revised 5 February 2021; editorial decision 29 May 2021; accepted 18 June 2021; online publish-ahead-of-print 23 June 2021

See page 4493 for the editorial comment for this article 'Assembling fats and sugar for cardiac protection', by J.-L. Balligand and L.Y.M.. Michel, https://doi.org/10.1093/eurheartj/ehab606.

Aims

Cardiac injury and remodelling are associated with the rearrangement of cardiac lipids. Glycosphingolipids are membrane lipids that are important for cellular structure and function, and cardiac dysfunction is a characteristic of rare monogenic diseases with defects in glycosphingolipid synthesis and turnover. However, it is not known how cardiac glycosphingolipids regulate cellular processes in the heart. The aim of this study is to determine the role of cardiac glycosphingolipids in heart function.

Methods and results

Using human myocardial biopsies, we showed that the glycosphingolipids glucosylceramide and lactosylceramide are present at very low levels in non-ischaemic human heart with normal function and are elevated during remodelling. Similar results were observed in mouse models of cardiac remodelling. We also generated mice with cardiomyocyte-specific deficiency in *Ugcg*, the gene encoding glucosylceramide synthase (h*Ugcg*$^{-/-}$ mice). In 9- to 10-week-old h*Ugcg*$^{-/-}$ mice, contractile capacity in response to dobutamine stress was reduced. Older h*Ugcg*$^{-/-}$ mice developed severe heart failure and left ventricular dilatation even under baseline conditions and died prematurely. Using RNA-seq and cell culture models, we showed defective endolysosomal retrograde trafficking and autophagy in *Ugcg*-deficient cardiomyocytes. We also showed that responsiveness to β-adrenergic stimulation was reduced in cardiomyocytes from h*Ugcg*$^{-/-}$ mice and that *Ugcg* knockdown suppressed the internalization and trafficking of β1-adrenergic receptors.

* Corresponding author. Tel: +46-31-3427578, Email: malin.levin@wlab.gu.se
The work was performed at the Department of Molecular and Clinical Medicine/Wallenberg Laboratory, Institute of Medicine, the Sahlgrenska Academy at University of Gothenburg and Sahlgrenska University Hospital.

Conclusions Our findings suggest that cardiac glycosphingolipids are required to maintain β-adrenergic signalling and contractile capacity in cardiomyocytes and to preserve normal heart function.

Graphical Abstract

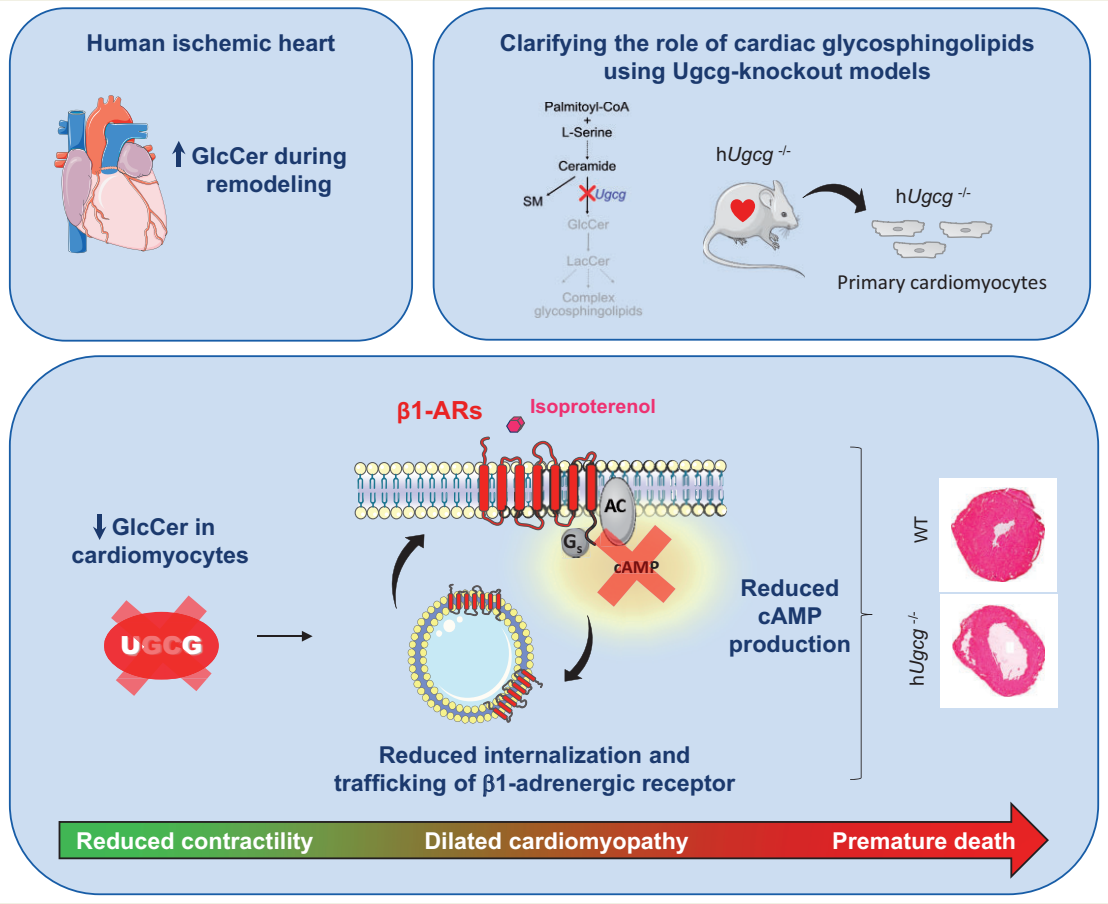

Cardiac glycosphingolipids are required to maintain β-adrenergic signaling and contractile capacity in cardiomyocytes and to preserve normal heart function.

Keywords Cardiac dysfunction • Lipids • Receptors • Adrenergic • Beta • Autophagy • Glycosphingolipids • Endolysosomal trafficking

Introduction

Progression of heart failure, a leading cause of death worldwide whose prevalence is increasing,[1] is associated with maladaptive ventricular remodelling in response to myocardial infarction or other cardiac injury.[2,3] This remodelling is characterized by an immediate enlargement of existing cardiomyocytes and increased left ventricular mass to compensate for the loss of contractile activity in the affected zone. Although remodelling likely confers short-term benefits, the left ventricle will expand and dilate over time, resulting in wall stress, ineffective contractile performance, and ultimately heart failure.[2,4]

Cardiac injury and remodelling are associated with changes in cardiac lipid composition.[5–8] Myocardial ischaemia has long been linked to cardiac triglycerides,[5] and we and others have shown that cardiac sphingolipids accumulate in the ischaemic heart.[7,9,10] Sphingolipids have also been implicated in cardiac disease. For example, several genome-wide association studies have linked genetic variants in sphingolipid (and especially glycosphingolipid) synthesis genes to the incidence of myocardial infarction.[11] In addition, cardiac dysfunction is a characteristic of rare monogenic diseases with defects in glycosphingolipid biosynthesis and turnover, such as Gaucher type III and Fabry (resulting in accumulation of glycosphingolipids in lysosomes).[12,13] However, studies of cardiac sphingolipids have mainly

Translational perspective

The molecular mechanisms that drive the progression of heart failure are poorly understood due to the complex and multifactorial nature of the disease. Emerging evidence indicates that cardiac injury and remodelling are associated with the rearrangement of cardiac lipid composition. In this study, we investigated the role of glycosphingolipids in heart function and found that cardiac glycosphingolipids are required to maintain β-adrenergic signalling and contractile capacity in cardiomyocytes and to preserve normal heart function. Thus, modulation of cardiac glycosphingolipids may represent a new promising inotropic therapeutic approach.

focused on the accumulation of lipotoxic ceramides after myocardial ischaemia and the effects of blocking sphingolipid synthesis to reduce ceramide accumulation.[14–16] It is not known whether downstream sphingolipids with a more structural function have a role in cardiomyocyte function.

Glycosphingolipids are membrane lipids that are important for cellular structure and function.[17,18] They are abundant in caveolae and lipid rafts,[19] which are central for receptor signalling and vesicular trafficking. Glycosphingolipids are synthesized in the Golgi apparatus. The first step, glucosylation of ceramide to form glucosylceramide (GlcCer), is catalysed by GlcCer synthase (encoded by *UGCG*).[20] GlcCer is the precursor of lactosylceramide (LacCer) and more complex glycosphingolipids.[18] The glucosylation of sphingolipids to generate glycosphingolipids alters the biophysical properties of cellular membranes[21]. Although glycosphingolipids play important roles in many cellular signalling pathways,[22,23] it is not known whether glycosphingolipids regulate cellular processes in the heart.

In this study, we investigated the role of cardiac glycosphingolipids in heart function. We used human left ventricular biopsies to determine the association between glycosphingolipids and heart function. Furthermore, we generated mice with cardiomyocyte-specific deficiency in glycosphingolipid synthesis (h*Ugcg*$^{-/-}$ mice) and cell culture models to ascertain how reduced levels of cardiac glycosphingolipids affect cardiac physiology and function.

Methods

A detailed description of all methods is provided in the Supplementary material online.

Human subjects

Cardiac biopsies were obtained from 44 cardiac surgery patients. All patients were examined preoperatively with echocardiography and the ejection fraction (EF) was measured. Non-ischaemic biopsies from the left ventricle were obtained from seven subjects undergoing aortic valve replacement, with angiography-verified absence of coronary artery disease in any major myocardial coronary artery branch, patient characteristics can be found in Supplementary material online, *Table S1*. Ischaemic biopsies were obtained from 37 patients undergoing coronary artery bypass surgery due to significant atherosclerotic stenosis in the epicardial coronary arteries. Coronary angiograms of these patients revealed multivessel disease including significant stenosis of left main and/or left anterior descending artery, patient characteristics can be found in Supplementary material online, *Table S2*. The patients were scored for severity of coronary artery disease, from 1 to 5 with increasing severity (1 = single-vessel disease, SVD; 2 = multivessel disease, MVD; 3 = left main, LM; 4 = LM + SVD; 5 = LM + MVD). The patients were divided into two groups according to their heart function; EF >55% ($n = 22$), which reflects a normal heart function and EF <45% ($n = 15$), which reflects a reduced heart function. The echocardiograms were analysed by an experienced senior consultant in cardiology with expertise in echocardiography and revealed that only four patients out of 20 with available echocardiography (20%) showed cardiac remodelling in the patient group with normal EF; while 9 out of 10 (90%) with available echocardiography showed remodelling in the patient group with low EF. Cardiac remodelling was defined as the presence of hypertrophy and/or left ventricular dilatation. In addition, area of hypokinesia/dyskinesia was identified, and myocardial biopsies were divided into remote, penumbra, or ischaemic (related to the affected myocardial territory). All biopsies were collected from the left ventricle septum region with a needle (1 mm). All samples were collected during cardiopulmonary bypass during cardiac arrest with aorta clamped and cardioplegia administered. All patients gave informed and written consent. The study was approved by the Gothenburg Regional Ethics Committee and done according to the Declaration of Helsinki.

Mice

All studies in mice were approved by the local animal Ethics Committee and conform to the guidelines from Directive 2010/63/EU of the European Parliament on the protection of animals used for scientific purposes. Mice were fed standard rodent chow (consisting of 12% calories from protein, 12% from fat, and 66% from carbohydrates) and housed in a pathogen-free barrier facility with a 12-h light/12-h dark cycle. All mice were bred on a C57BL/6N (Taconic) background.

Ugcg$^{fl/fl}$ mice,[24] in which exons 6 and 7 were flanked with loxP sites, and α-myosin heavy chain (α-MHC)-Cre mice (stock no. 009074, Jackson Laboratories) were crossbred to generate cardiomyocyte-specific *Ugcg* knockdown h*Ugcg*$^{-/-}$ mice (*Ugcg*$^{fl/fl}$/α-MHC-Cre) and littermate h*Ugcg*$^{+/+}$controls (*Ugcg*$^{fl/fl}$). In some experiments, heterozygotic *Ugcg* mice (*Ugcg*$^{fl/-}$/α-MHC-Cre) and their littermate controls (*Ugcg*$^{fl/-}$) were also used. Genomic DNA from various tissues was analysed by PCR, and genotyping was done from ear snip biopsies and re-confirmed post-mortem as described.[24] Primers for genotyping are listed in Supplementary material online, *Table S3*. Experiments were performed in 9- to 10-week-old mice unless otherwise stated. After the experiments, fasted mice were anaesthetized with isoflurane and killed by cervical dislocation. Unless otherwise stated, hearts and other tissues were removed, rinsed in phosphate-buffered saline, snap-frozen in liquid N_2, and stored at –80°C until analysis.

Isoproterenol-stimulated cAMP production

A detailed description of the method is provided in the Supplementary material online. In short, primary cardiomyocytes, HEK-293 and HEK-β1AR cells were stimulated with the indicated concentration of isoproterenol in culture medium supplemented with IBMX (100 μM) and ascorbic acid (10 μM), for 10 min at 37°C. Thereafter, the cells were harvested, and intracellular levels of cAMP were measured with the Parameter cAMP kit (R&D Systems) according to the manufacturer's instructions.

Statistical analysis

Values are reported as means ± SD. Data distribution within all separate groups were validated by the Anderson–Darling or Shapiro–Wilk normality test. Parametric unpaired two-tailed *t*-test was used for comparisons of two groups, if the normality test was not passed the non-parametric Mann–Whitney test was used. ANOVA followed by Tukey's multiple comparisons test (alpha 0.05) was used for comparison of more than two groups, if normality test was not passed the non-parametric Kruskal–Wallis test was performed. Survival was assessed with the log-rank test. $P < 0.05$ was considered statistically significant. GraphPad Prism Software was used for all statistical analyses.

Results

Glycosphingolipid levels increase in the remodelling heart

Ugcg, the gene encoding GlcCer synthase (which catalyses the first step of glycosphingolipid synthesis, see *Figure 1A* for schematic overview), is expressed in most tissues; its expression is highest in bone marrow, dendritic cells, and adrenal gland and much lower in cardiac tissues in humans (Consensus dataset,[25] www.proteinatlas.org (28 June 2021)). By profiling membrane lipids in human non-ischaemic left ventricular tissues, we showed that the glycosphingolipids GlcCer and LacCer were indeed present in human cardiac tissue, but at lower levels than other membrane lipids (*Table 1*). GlcCer, but not LacCer, concentrations were higher in left ventricular biopsies from patients with reduced EF than in those with normal heart function after chronic ischaemia (*Figure 1B and C*). However, glycosphingolipid levels did not correlate with the severity of coronary artery disease (Supplementary material online, *Figure S1*) or with the affected myocardial territory (Supplementary material online, *Figure S2*).

To confirm that glycosphingolipids are increased in the remodelling heart, we induced cardiac remodelling in mice by inducing a myocardial infarction or by injecting the non-selective β-adrenoceptor (βAR) agonist isoproterenol. After the myocardial infarction, cardiac GlcCer and LacCer levels were increased at both 24 and 72 h (*Figure 2A and B*); GlcCer levels were higher both near the scar region (left ventricle) and in remote regions (ventricular septum and atrium) (*Figure 2A*) but LacCer levels were increased only near the scar region (*Figure 2B*). At 24 h after isoproterenol injection, GlcCer levels were increased in the atrium, but not in the left ventricle, and LacCer levels were not altered (*Figure 2C and D*). Full lipidomics and metabolomics profiles are included in Supplementary material online, *Figure S3* and *Tables S4–S7*.

Cardiomyocyte-specific *Ugcg* depletion causes dilated cardiomyopathy and early death

To investigate whether glycosphingolipids have a role in cardiac function, we generated mice with cardiomyocyte-specific deficiency in *Ugcg*. PCR analyses of genomic DNA from these h*Ugcg*$^{-/-}$ mice showed depletion of *Ugcg* in heart tissue and isolated cardiomyocytes, but not in skeletal muscle, liver, lung, spleen, white adipose tissue, or cardiac fibroblasts (Supplementary material online, *Figure S4A and B*). *Ugcg* transcript levels were consistently reduced by 64% in cardiac tissue and 88% in isolated cardiomyocytes but were not affected in liver, skeletal muscle, lung, spleen, white adipose tissue, and isolated macrophages (Supplementary material online, *Figure S4C and D*). LacCer levels were reduced in cardiac tissue, and both GlcCer and LacCer levels were markedly reduced in cardiomyocytes from h*Ugcg*$^{-/-}$ mice (Supplementary material online, *Figure S4E and F*). Cardiomyocyte-specific depletion of *Ugcg* did not affect body weight (Supplementary material online, *Figure S5*) or plasma levels of glucose, insulin, or lipids (Supplementary material online, *Table S8*). h*Ugcg*$^{-/-}$ mice had normal heart volume, dimensions, and function under basal conditions at 9–10 weeks of age (*Figure 3A*). However, cardiomyocyte-specific deletion of *Ugcg* in 9- to 10-week-old mice resulted in (i) higher cardiac mRNA expression of markers for

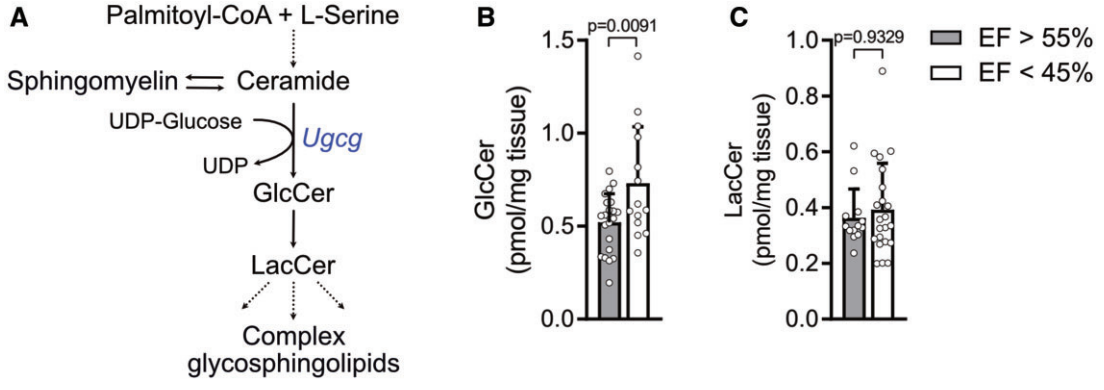

Figure 1 Glucosylceramide levels are increased in the remodelling human heart. (*A*) Schematic picture of the *de novo* biosynthesis pathway of glycosphingolipids. (*B*) GlcCer and (*C*) LacCer levels in left ventricular biopsies from patients after an ischaemic event with normal ejection fraction (>55%) or reduced ejection fraction (<45%) ($n = 22$ for ejection fraction >55% and $n = 15$ for ejection fraction <45%). Values are mean ± SD, two-tailed Student's *t*-test for *B*, and Mann–Whitney non-parametric test for *C*.

Table 1 Membrane lipid levels in human non-ischaemic left ventricular biopsies, from patients undergoing aortic valve replacement

Lipid	pmol/mg tissue
PC	7206 ± 3494
SM	994 ± 465
PE	1806 ± 1032
Cer	8.21 ± 3.88
DiCer	0.26 ± 0.11
GlcCer	0.49 ± 0.24
LacCer	0.34 ± 0.12

Data are mean ± SD ($n = 7$).
Cer, ceramide; DiCer, dihydroceramide; GlcCer, glucosylceramide; LacCer, lactosylceramide; PC, phosphatidylcholine; PE, phosphatidylethanolamine; SM, sphingomyelin.

cardiac dysfunction and fibrosis, namely *Nppa* and *Nppb*, which encode atrial natriuretic peptide and B-type natriuretic peptide (BNP), and *Timp1* and *Ctgf*, which encode the extracellular matrix regulators tissue inhibitor of metalloproteinase 1 and connective tissue growth factor (*Figure 3B*); and (ii) lower cardiac expression of known contractility markers (*Figure 3C*). Immunohistochemistry revealed emerging fibrosis in sections from h*Ugcg*$^{-/-}$ mice (Supplementary material online, *Figure S6*). Humoural factors, such as plasma noradrenaline and BNP, were not significantly increased (*Figure 3D*). Furthermore, when 9- to 10-week-old mice were injected with the β1AR agonist dobutamine to induce physiological cardiac stress, diastolic and systolic volumes were higher, relative wall thickness was lower and velocity of circumferential fibre shortening was lower in h*Ugcg*$^{-/-}$ mice than in h*Ugcg*$^{+/+}$ mice (*Figure 3E*, Supplementary material online, *Figure S7*), indicating that the contractile capacity of young h*Ugcg*$^{-/-}$ mice is compromised during stress.

At 6 months of age, h*Ugcg*$^{-/-}$ mice had pronounced characteristics of cardiomyopathy even under baseline conditions, with enlarged hearts and LV dilatation (*Figure 4A*), profound fibrosis, cardiomyocyte disarray, and glycogen accumulation (*Figure 4B*). Heart weight and ventricular dimension were increased (*Figure 4C and D*) and EF was severely reduced. Lung weight was also increased (*Figure 4E*), indicating pulmonary congestion and heart failure. Circulation noradrenaline was slightly increased (*Figure 4F*). The pronounced cardiac failure resulted in premature death, with a mortality rate of 80% at 40 weeks, as shown by Kaplan–Meier plot (*Figure 4G*). Of note, cardiomyocytes from mice lacking one copy of *Ugcg* (h*Ugcg*$^{fl/-}$ mice) also had significantly reduced levels of GlcCer and LacCer, markedly impaired heart function, and increased heart and lung weight (Supplementary material online, *Figure S8*).

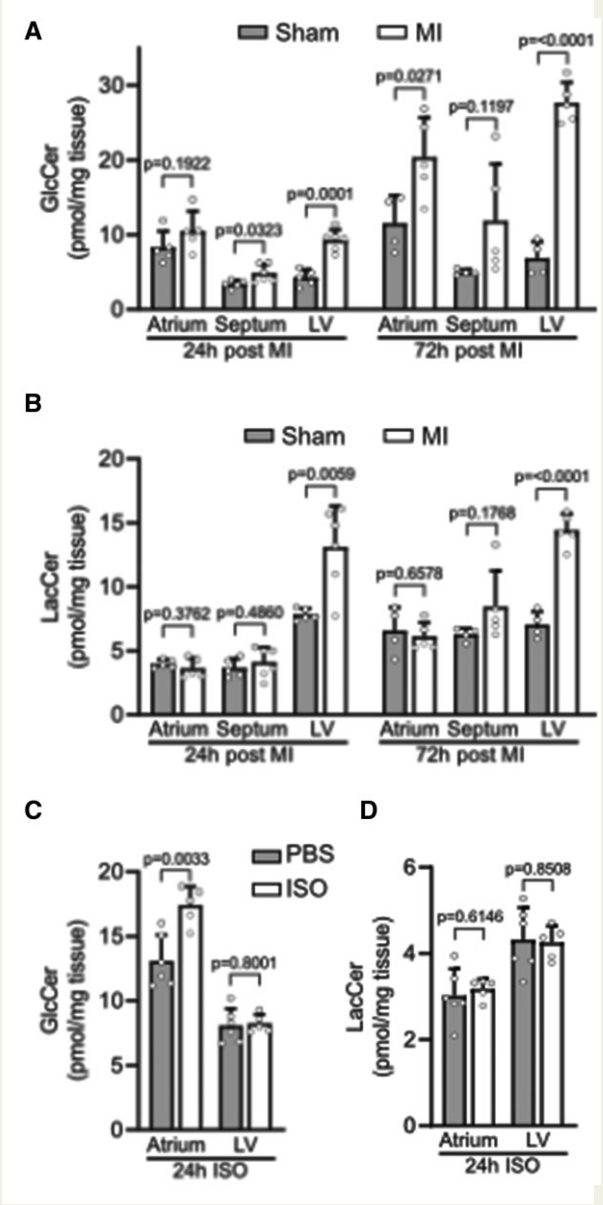

Figure 2 Glucosylceramide levels are increased in the remodelling mouse heart. GlcCer (*A*) and LacCer levels (*B*) in the scar region (left ventricle) and in the proximal region (atrium and ventricular septum) of the mouse heart 24 and 72 h after a myocardial infarction ($n = 4$–6). GlcCer levels (*C*) and LacCer levels (*D*) in the atrium and left ventricle 24 h after an isoproterenol (ISO) injection (30 mg/kg) ($n = 5$–6). Values are mean ± SD, two-tailed Student's *t*-test. GlcCer, glucosylceramide; LacCer, lactosylceramide.

Transcriptomics reveals defects in trafficking processes in *Ugcg*-deficient cardiomyocytes

To gain insight into molecular mechanisms of the heart failure in h*Ugcg*$^{-/-}$ mice, we did whole-genome RNA sequencing (RNA-seq) on cardiomyocytes with chronic *Ugcg*$^{-/-}$ deficiency (isolated from h*Ugcg*$^{-/-}$ mice and littermate controls at 8 weeks of age) and acute *Ugcg*$^{-/-}$ deficiency (cultured HL-1 cardiomyocytes depleted of *Ugcg* with siRNA, Supplementary material online, *Figure S9*). The RNA-seq analysis of cardiomyocytes with chronic *Ugcg*$^{-/-}$ deficiency indicated striking and widespread signs of marked contractile dysfunction, with severe defects in contractile elements and calcium handling (Supplementary material online, *Figure S10*).

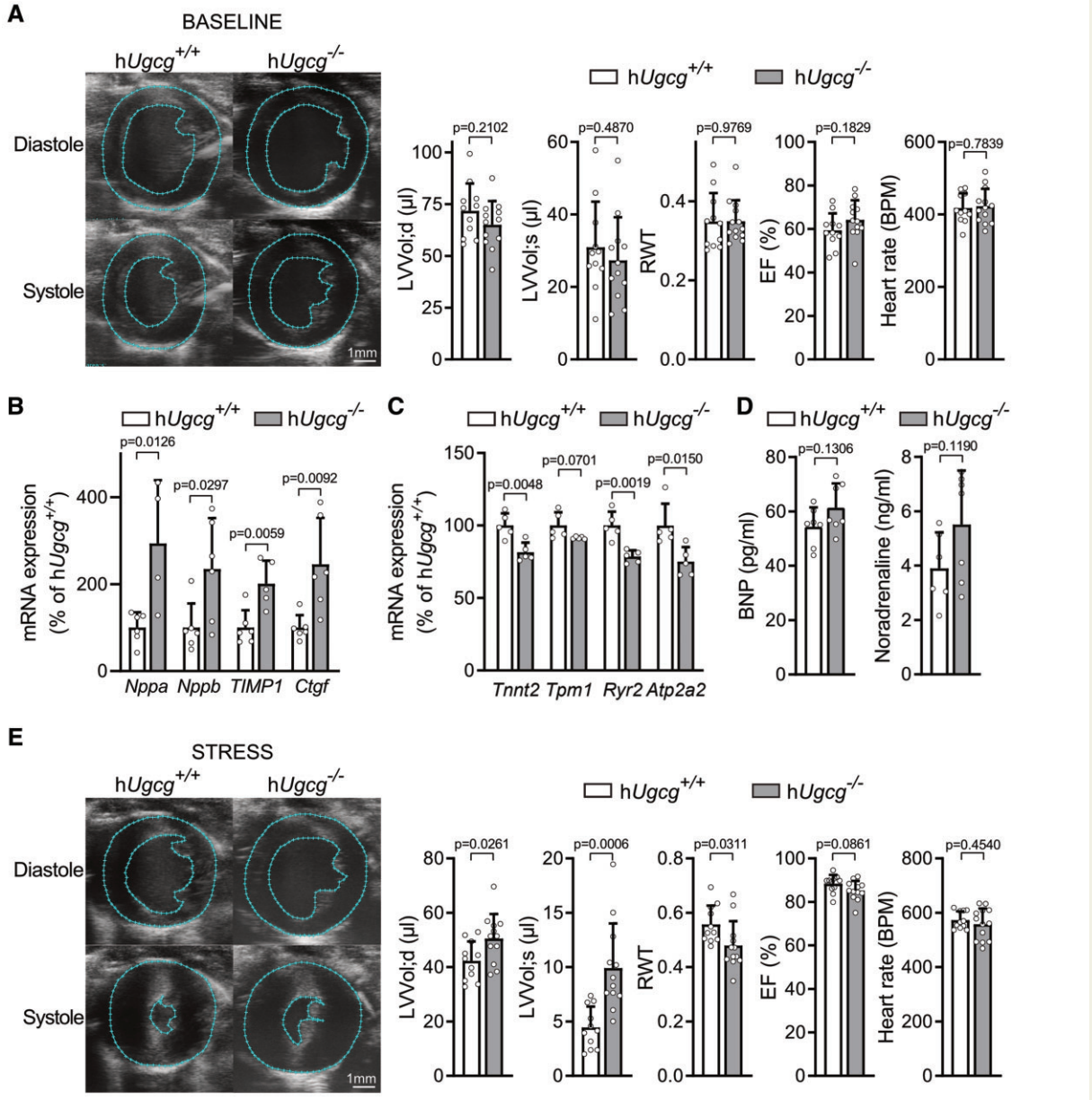

Figure 3 Normal heart function at baseline but reduced heart function after dobutamine stress in 9- to 10-week-old h*Ugcg*$^{-/-}$ mice. (*A*) Cardiac function and heart rate in h*Ugcg*$^{+/+}$ and h*Ugcg*$^{-/-}$ mice at 9–10 weeks of age under baseline conditions assessed with echocardiography ($n = 11$ h*Ugcg*$^{+/+}$, $n = 12$ h*Ugcg*$^{-/-}$). (*B*) mRNA expression of atrial natriuretic peptide (ANP, *Nppa*), B-type natriuretic peptide (*Nppb*), tissue inhibitor of metalloproteinase 1, and connective tissue growth factor in the hearts of 9- to 10-week-old h*Ugcg*$^{+/+}$ and h*Ugcg*$^{-/-}$ mice ($n = 5$/group). (*C*) mRNA expression of *Tnnt2, Tpm1, Ryr2*, and *Atp2a2* in the hearts of 9- to 10-week-old h*Ugcg*$^{+/+}$ and h*Ugcg*$^{-/-}$ mice ($n = 5$ per group). (*D*) Plasma B-type natriuretic peptide and noradrenaline levels in 9- to 10-week-old h*Ugcg*$^{+/+}$ and h*Ugcg*$^{-/-}$ mice ($n = 7$ per group). (*E*) Cardiac function and heart rate in h*Ugcg*$^{+/+}$ and h*Ugcg*$^{-/-}$ mice at 9–10 weeks of age after dobutamine stress assessed with echocardiography ($n = 11$–12). Values are mean ± SD, two-tailed Student's *t*-test for *A, B, C*, and *E*, and Mann–Whitney non-parametric test for *D*. BPM, beats per minute; EF, ejection fraction; LVVol; d, left ventricular volume in diastole; LVVol; s, left ventricular volume in systole; RWT, relative wall thickness.

However, these results most likely reflect emerging cardiac dysfunction rather than direct effect of glycosphingolipid depletion. The RNA-seq analysis of cardiomyocytes with acute *Ugcg*$^{-/-}$ deficiency identified 287 genes whose mRNA levels differed significantly from those in control cardiomyocytes. Gene Ontology and Kyoto Encyclopedia of Genes and Genome pathway analyses revealed that *Ugcg* knockdown markedly reduced levels of mRNAs that help regulate cellular trafficking processes, such as protein

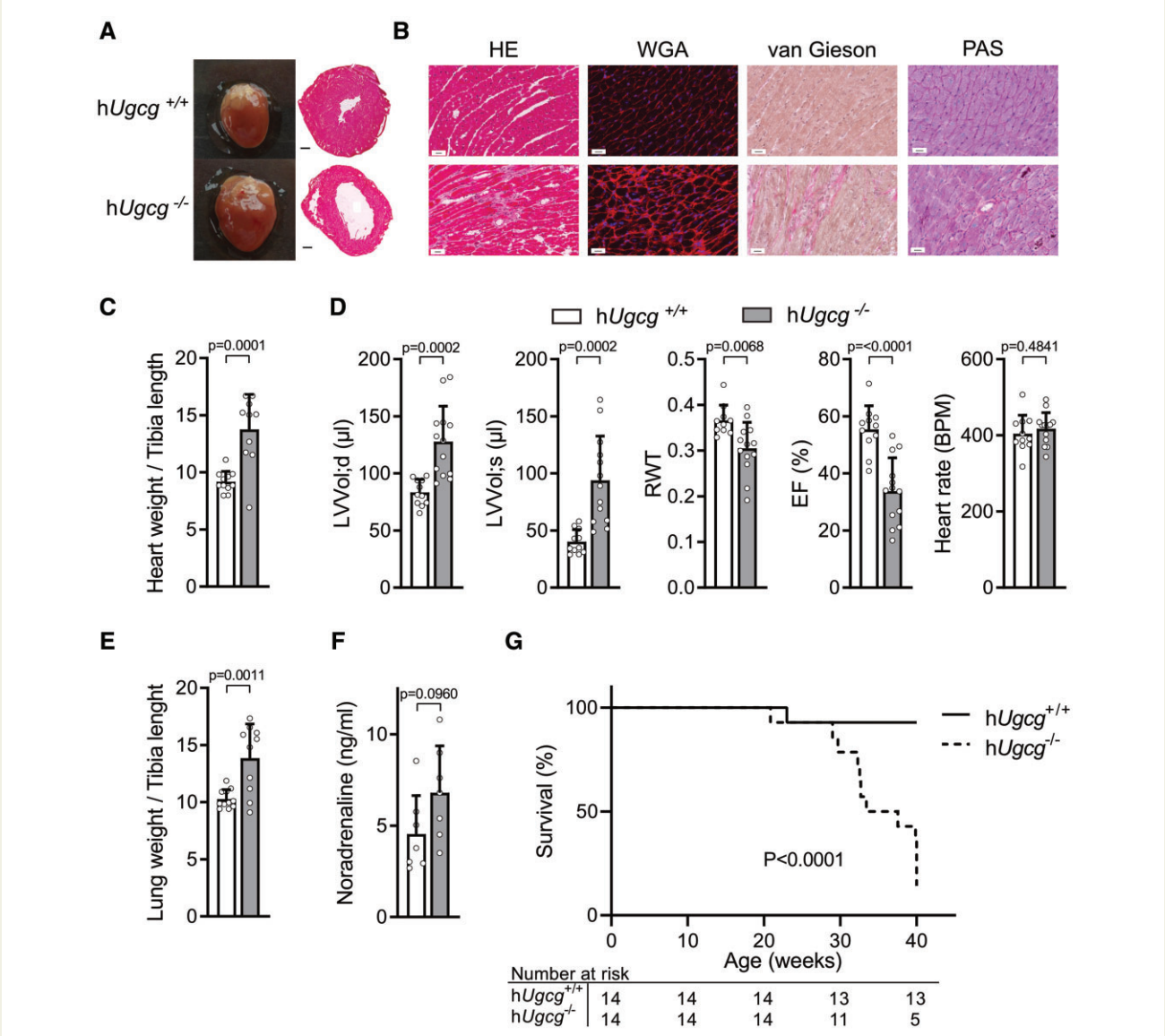

Figure 4 Cardiomyocyte-specific deletion of *Ugcg* results in dilated cardiomyopathy and premature death. (*A*) Representative photographs (left) and haematoxylin/eosin (H&E)-stained sections (right) of hearts of 30-week-old h*Ugcg*$^{+/+}$and h*Ugcg*$^{-/-}$ mice. Scale bar, 500 µm. (*B*) Representative haematoxyin/eosin-stained sections shows fibrosis (pink) and cardiomyocyte disarray, wheat germ agglutinin (WGA) staining shows cardiomyocyte disarray, van Gieson staining shows fibrosis (red), and periodic acid–Schiff (PAS) staining shows glycogen accumulation (magenta) in cross-sections of hearts from 30-week-old h*Ugcg*$^{+/+}$ mice (upper panel) and h*Ugcg*$^{-/-}$ mice (lower panel). Scale bar, 20 µm. (*C*) Heart weight/tibia length of 30-week-old h*Ugcg*$^{+/+}$and h*Ugcg*$^{-/-}$ mice ($n = 10–11$). (*D*) Cardiac function and heart rate in 26-week-old h*Ugcg*$^{+/+}$ and h*Ugcg*$^{-/-}$ mice assessed with echocardiography ($n = 11–12$). (*E*) Lung weight/tibia length of 30-week-old h*Ugcg*$^{+/+}$and h*Ugcg*$^{-/-}$ mice ($n = 10–11$). (*F*) Plasma noradrenaline levels in 26-week-old h*Ugcg*$^{+/+}$ and h*Ugcg*$^{-/-}$ mice ($n = 7$ per group) G, Kaplan–Meier survival curves of h*Ugcg*$^{+/+}$and h*Ugcg*$^{-/-}$ mice ($n = 14$). Values are mean ± SD, two-tailed Student's *t*-test.

transport, transmembrane transport, retrograde protein transport, endoplasmic reticulum (ER)-to-cytosol transport, and processes involving the lysosome (*Figure 5*). We validated some of our identified pathways in the non-ischaemic human heart and compared it with ischaemic human heart (Supplementary material online, *Figure S11*). Our dataset revealed that the LV tissue of patients with ischaemic heart disease had up-regulation of genes involved in the protein targeting to the membrane and protein localization to the ER biological processes (i.e. the opposite direction that we found in h*Ugcg*$^{-/-}$ hearts); whereas there was down-regulation of genes involved in cellular components such as the ER to Golgi transport vesicle membrane and COPII coated ER to Golgi transport vesicle. Thus, our results suggest that pathways involving cellular trafficking are sensitive to

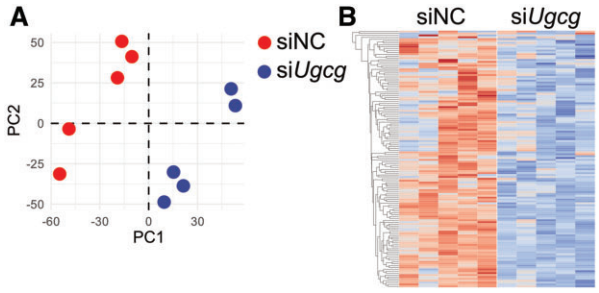

Biological Process		Mean Fold-Change (Down-regulated)*
[GO-BP]	Protein transport	-3.15
[GO-BP]	Transmembrane transport	-3.94
[GO-BP]	Retrograde protein transport	-2.58
[GO-BP]	ER to cytosol transport	-3.00
[KEGG]	Lysosome	-3.73

Figure 5 Transcriptomics reveals defects in trafficking processes in *Ugcg*-deficient cardiomyocytes. Whole-genome RNA sequencing was done on HL1 cardiomyocytes treated with siRNA against Ugcg (siUgcg) or scrambled control (siNC). (*A*) PCA plot of each sample from control cells and Ugcg-depleted HL1 cardiomyocytes. Depletion of *Ugcg* significantly affected the transcriptomic profile, as shown by clear separation of both groups ($n = 5$ per group). (*B*) Left: Heatmap of the transcripts per million (TPM) relative values (Z-score normalized) of significantly down-regulated genes in each sample from control and Ugcg-depleted HL1 cardiomyocytes. Right: List of significantly down-regulated Gene Ontology biological processes and Kyoto Encyclopedia of Genes and Genome pathways related to cellular trafficking in Ugcg-depleted cardiomyocytes vs. control cells. *Retrieved from gene set statistics from Piano analysis.

alterations (both up- and down-regulation) in glycosphingolipid metabolism.

Endolysosomal function and autophagy are impaired in *Ugcg*-deficient cardiomyocytes

Since the RNA-seq analysis showed profound alterations in cellular trafficking, we first investigated whether glycosphingolipid depletion in cardiomyocytes affects cellular anterograde trafficking. The transport of the temperature-sensitive VSVG-GFP protein through the trans-Golgi network to the plasma membrane did not differ between *Ugcg*-depleted and control HL-1 cardiomyocytes, indicating that *Ugcg* deficiency does not affect anterograde transport in these cells (*Figure 6A*).

Next, we investigated whether glycosphingolipid depletion in HL-1 cardiomyocytes affects organelles and structures involved in retrograde transport. We assessed syntaxin 5 (Stx5), a marker of endosome-to-Golgi transport[26] and of Golgi assembly[27]; GM130, a *cis*-Golgi matrix protein; and TGN46, a *trans*-Golgi matrix protein by western blot. Acute depletion of *Ugcg* significantly reduced GM130 and Stx5 levels, but did not affect the level of TGN46 (*Figure 6B*), and also resulted in dispersed Golgi (*Figure 6C*), which were clearly visible by electronic microscopy in hearts from young h*Ugcg*$^{-/-}$ mice (*Figure 6D*). Further analysis revealed that structures positive for LAMP1, a marker of endolysosomal organelles, were smaller in *Ugcg*-depleted cardiomyocytes (*Figure 6E*). In the presence of chloroquine, an inhibitor of lysosome-autophagosome fusion,[28] *Ugcg*-depleted cardiomyocytes had less LAMP1 staining and smaller LAMP1-positive organelles than control cells (*Figure 6E*); the marked reduction in LAMP1 staining was confirmed by western blot analysis (*Figure 6F*), suggesting impaired endolysosomal function. Thus, glycosphingolipid depletion in cardiomyocytes results in defects in endolysosomal trafficking and in Golgi dispersion.

To determine whether the reduction in glycosphingolipids affects autophagy, we assessed LC3B as a marker of autophagosomes. Very few LC3B-positive puncta were visible in control and *Ugcg*-depleted cardiomyocytes under baseline conditions (*Figure 6E*). In the presence of chloroquine, however, LC3B-positive organelles accumulated in control cardiomyocytes but were reduced in *Ugcg*-depleted cardiomyocytes (*Figure 6E*). Western blot analysis showed a reduction of LC3BII in *Ugcg*-depleted HL-1 cardiomyocytes both in the absence and presence of chloroquine (*Figure 6F*; Supplementary material online, *Figure S12*). Evidently, autophagy is reduced in cardiomyocytes with reduced glycosphingolipid levels.

Hyperactivation of mTORC1, a negative regulator of autophagy,[29] has been proposed to promote down-regulation of lysosomal functions.[30] During stress, mTOR is inhibited (by phosphorylation at S2448), leading to activation of the autophagy-initiating kinase ULK1 (by phosphorylation at S757). Depletion of *Ugcg* increased the phosphorylation of mTOR at S2448, of ULK1 at S757, and of the mTORC1 downstream target p70S6K, as shown by western blot analysis (*Figure 6G*). These results suggest that low glycosphingolipid levels lead to activation of mTORC1 and ultimately to reduced induction of the autophagy process.

Collectively, our findings indicate that the anterograde transport system is intact, but the retrograde transport system, including endolysosomal and autophagic processes, are compromised in glycosphingolipid-depleted cardiomyocytes.

Ugcg-deficiency results in defective β-adrenergic receptor internalization and trafficking

Since contractile capacity after injection of a β1AR agonist was lower in young h*Ugcg*$^{-/-}$ mice than in young h*Ugcg*$^{+/+}$ mice (*Figure 3E*), we hypothesized that responsiveness to β-adrenergic stimulation is impaired in glycosphingolipid-deficient cardiomyocytes, potentially through an effect on receptor trafficking.

First, we showed that cAMP generation induced by a βAR agonist (isoproterenol) was markedly lower in cardiomyocytes from h*Ugcg*$^{-/-}$ mice than in those from littermate controls (*Figure 7A and B*),

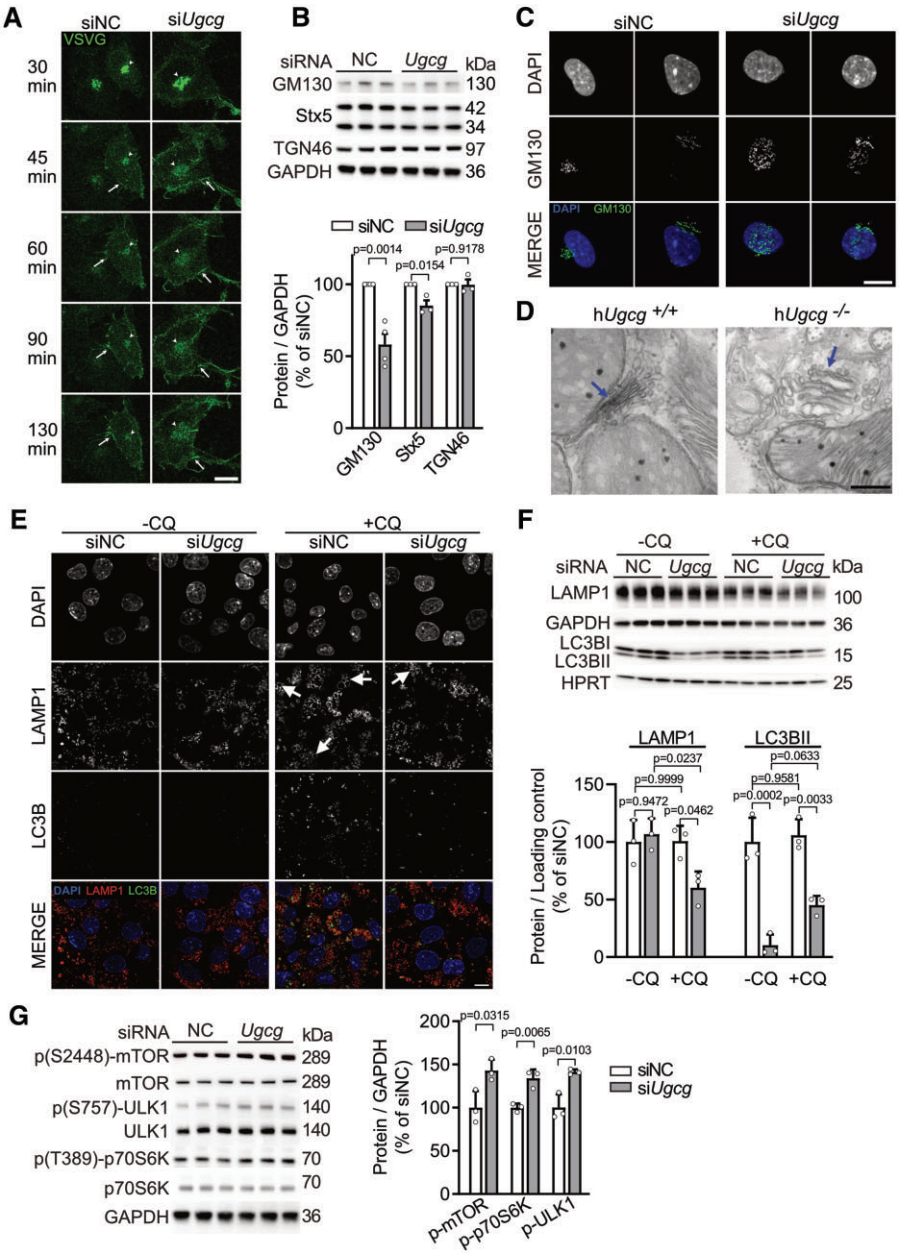

Figure 6 *Ugcg*-deficient cardiomyocytes have impaired endolysosomal function and autophagy. (*A*) Representative confocal images of VSVG-GFP transport in normal control (NC) and Ugcg-depleted HL1 cardiomyocytes at the indicated time after temperature shift (40°C to 32°C). Arrows indicate plasma membrane localization. Arrowheads indicate Golgi localization in siRNA-transfected cells. Scale bar, 20 μm. (*B*) Representative immunoblot images and quantification of GM130, Stx5, and TGN46 in Ugcg-depleted HL1 cells; GAPDH served as the loading control. Values are mean ± SD, of three separate experiments, two-tailed Student's *t*-test. (*C*) Representative immunostaining images of GM130 (green) in Ugcg-depleted HL1 cells. Scale bar, 20 μm. (*D*) Electron microscopy images of primary cardiomyocytes from h*Ugcg*$^{+/+}$ and h*Ugcg*$^{-/-}$ mice. Arrows indicate Golgi structures. Scale bar, 500 nm. (*E*) Representative immunostaining images of LAMP1 (red) and LC3B (green) in Ugcg-depleted HL1 cells treated with chloroquine (CQ) (25 μM) or left untreated. Scale bar, 10 μm. Arrow indicates representative LAMP1-positive endolysosomes with a diameter of 2 μm. Percentage of cells containing LAMP1-positive endolysosomes with a diameter of >2 μm (at least three per cell): siNC-CQ, 13.12%; siUgcg-CQ, 11.91%; siNC+CQ, 62.16%; and siUgcg+CQ, 31.75% (n = 37–63 cells from one randomly chosen field). (*F*) Representative immunoblot images and quantification of LAMP1 and LC3BII in Ugcg-depleted, serum-starved HL1 cells treated with chloroquine (25 μM) or left untreated. GAPDH served as loading control. Values are mean ± SD, n = 3, two-way ANOVA. (*G*) Representative immunoblot images and quantification of proteins in the mammalian target of rapamycin (mTOR) signalling pathway in Ugcg-depleted, serum- and amino acid-starved HL1 cells. GAPDH served as loading control. Values are mean ± SD, n = 3, two-tailed Student's *t*-test.

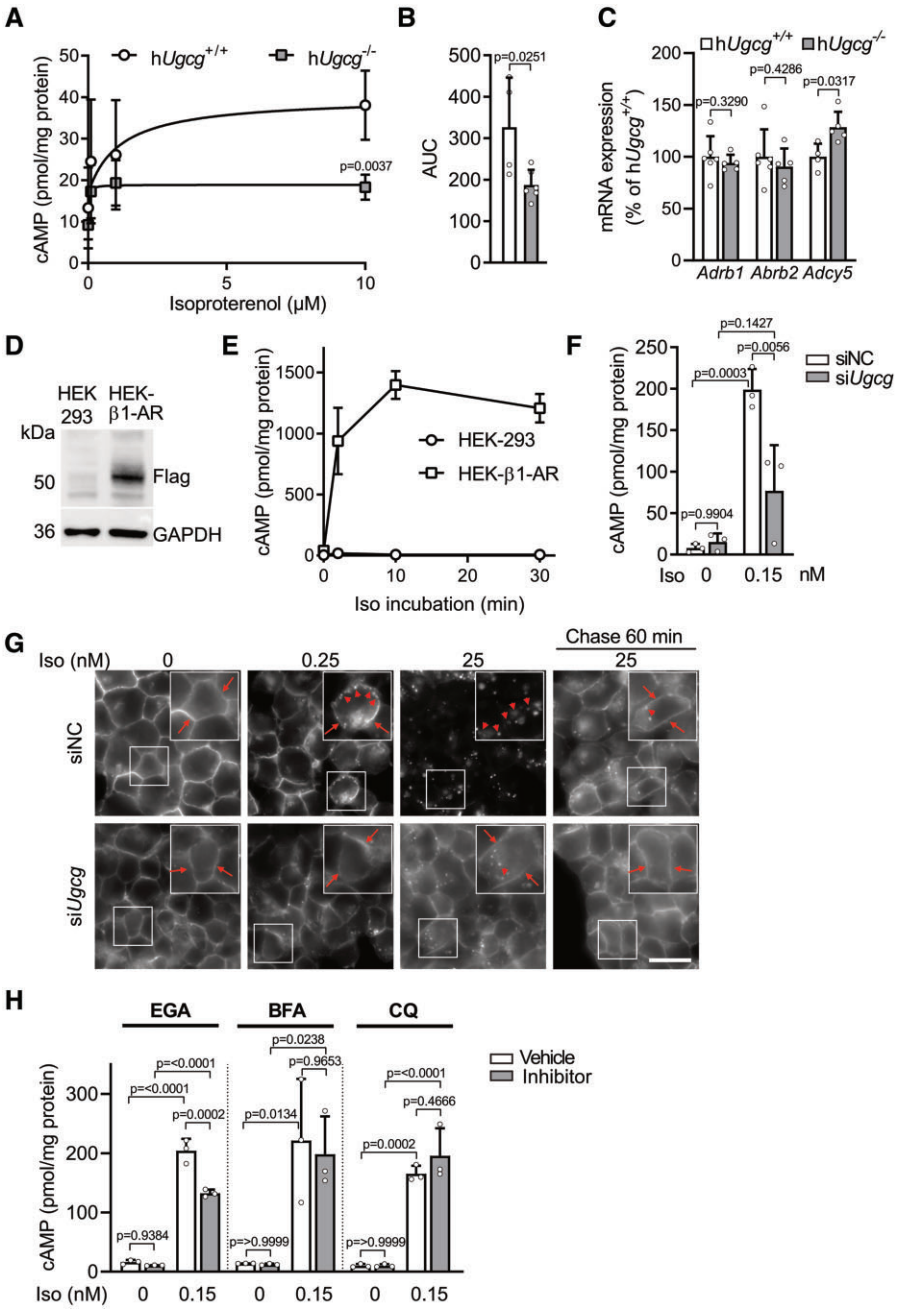

Figure 7 Loss of *Ugcg* in cardiomyocytes results in reduced responsiveness to β1-adrenergic receptor (β1AR) signalling. (*A*) Production of cAMP in primary cardiomyocytes from 9- to 10-week-old h*Ugcg*$^{+/+}$ and h*Ugcg*$^{-/-}$ mice ($n = 4$ h*Ugcg*$^{+/+}$, $n = 6$ h*Ugcg*$^{-/-}$) after 10 min of isoproterenol stimulation and IBMX (0.1 mM) treatment (two-way ANOVA followed by Tukey's *post hoc* test). (*B*) Quantification of cAMP production. AUC, area under the curve. Values are mean ± SD, $n = 3$, two-tailed Student's *t*-test. (*C*) mRNA expression of mRNA expression of *Adrb1*, *Adrb2*, and *Adcy5* in the hearts of 9- to 10-week-old h*Ugcg*$^{+/+}$ and h*Ugcg*$^{-/-}$ mice, $n = 4$–6. Values are mean ± SD, Mann–Whitney non-parametric test. (*D*) Immunoblot analysis of cell lysate from HEK293 cells and cells stably overexpressing β1AR (HEK-β1AR). GAPDH served as loading control. (*E*) Isoproterenol (1 μM) induced cAMP production in HEK293 cells, and HEK-β1AR cells treated with IBMX (0.1 mM) ($n = 2$ per time point). (*F*) Isoproterenol (0.15 nM) stimulated cAMP production in HEK-β1AR cells treated with IBMX (0.1 mM) and siRNA against Ugcg or scrambled control. Values are mean ± SD of three separate experiments, two-way ANOVA followed by Tukey's *post hoc* test. (*G*) Representative immunofluorescence images of the subcellular location of Flag-β1AR in HEK-β1AR cells treated with siRNA against Ugcg or scrambled control after a 30-min treatment with isoproterenol (Iso). After the treatment, cells were washed and incubated for 60 min (chase) to follow the recycling of the β1AR. Arrows indicate plasma membrane. Arrowheads indicate internalized receptor. (*H*) Isoproterenol (0.15 nM) stimulated cAMP production in IBMX-treated HEK-β1AR cells after a 1-h pre-treatment with EGA (25 μM, DMSO as vehicle), BFA (1 μg/mL, ethanol as vehicle), or CQ (25 μM, H_2O as vehicle). Values are mean ± SD, $n = 3$, two-way ANOVA followed by Tukey's *post hoc* test. β1AR, beta-1 adrenergic receptor.

indicating a reduced responsiveness to β-adrenergic stimulation. The reduced cAMP production is not due to reduced mRNA expression of significant players of the βAR-signalling system, such as β1AR (*adrb1*), β2AR (*adrb2*) or adenylate cyclase 5 (*adcy5*) (*Figure 7C*). To further analyse the potential effects of altered glycosphingolipid concentrations on β-adrenergic signalling, we established HEK293 cells that stably overexpress the β1AR (HEK-β1AR cells) (*Figure 7D*), a well-established model system for βAR-signalling.[31–34] Incubation with isoproterenol markedly increased cAMP generation in these cells (*Figure 7E*) and knockdown of *Ugcg* acutely reduced this response (*Figure 7F*). These results suggest that the reduced responsiveness of h*Ugcg*$^{-/-}$ cardiomyocytes to isoproterenol is a direct effect of *Ugcg* deficiency.

The β1AR is mainly localized in the plasma membrane and is rapidly desensitized and internalized by endocytosis upon agonist stimulation. The receptor is then either resensitized and recycled back to the plasma membrane by the endolysosomal trafficking system or degraded.[35] Disturbance of any of these steps would impair receptor signalling. Immunohistochemistry showed clear localization of the β1AR under basal conditions, with no differences between control and *Ugcg*-depleted HEK-β1AR cells (*Figure 7G*). In response to 25 nM isoproterenol, the β1AR was internalized in the control cells but not in *Ugcg*-depleted cells (*Figure 7G*). After wash out of the agonist and 60 min of chase, the receptor was again visible in the plasma membrane in the control cells (*Figure 7G*). To further clarify the localization of the β1AR, we studied the co-localization of the receptor with endosomal markers. Notably, we found that upon stimulation with isoproterenol in control cells, the β1AR internalized to the early endosome (as shown by co-localization with the early endosome marker early endosome antigen 1), but the β1AR did not localize to the late endosome (shown with the late endosome marker Rab7). In *Ugcg*-depleted cells, however, the main part of the β1ARs maintained on the plasma membrane upon isoproterenol stimulation, and no co-localization with early endosomes was detected (Supplementary material online, *Figure S13*).

To verify that the observed defects in endolysosomal trafficking in *Ugcg*-depleted cells in fact lead to the defective β1AR-internalization and signalling, we assessed cAMP production in the presence of diverse inhibitors of endolysosomal trafficking. Indeed, pre-incubation with EGA, a selective inhibitor of endolysosomal trafficking between the early and late endosome, lead to a significant decrease in the production of cAMP in a similar extent to the one observed upon *Ugcg* depletion . However, pre-incubation with brefeldin A (BFA), which is known to disintegrate the Golgi apparatus and inhibit the retrograde transport to the ER, or chloroquine (CQ), an inhibitor of the autophagy process that also has been shown to disorganize the Golgi and endolysosomal systems, did not affect the isoproterenol inducted cAMP production (*Figure 7H*). Thus, these results show that the impaired β1-adrenerigic signalling seen in *Ugcg*-depleted cardiomyocytes is a consequence of defect endolysosomal trafficking.

In sum, our results suggest that β1AR internalization and recycling is defective in *Ugcg*-deficient cells. Once activated, β1ARs in the plasma membrane are desensitized but are not internalized by endocytosis, resulting in reduced responsiveness to further β-adrenergic stimulation.

Discussion

This study shows that the glycosphingolipids GlcCer and LacCer are present at very low levels in the non-ischaemic human heart, but are markedly elevated in ischaemic heart disease with left ventricular dysfunction and remodelling. To define the role of glycosphingolipids in cardiac physiology and function, we generated mice with cardiomyocyte-specific depletion in glycosphingolipids (h*Ugcg*$^{-/-}$ mice) and observed a dramatic phenotype—dilated cardiomyopathy and premature death. Mechanistically, we showed that *Ugcg*-deficiency results in defective endolysosomal function and autophagy, leading to severely compromised β-adrenergic signalling. Thus, our findings suggest that an increased level of glycosphingolipids in the remodelling heart is a compensatory, beneficial response to facilitate remodelling and that glycosphingolipids are required to maintain cardiomyocyte structure and function and to preserve normal heart function (*Graphical abstract*).

Glycosphingolipids are membrane lipids that are important for cellular structure and function.[17,18] The first step of glycosphingolipid synthesis is the glucosylation of ceramide to form GlcCer, which in turn is the precursor of 300–400 glycosphingolipids.[22] Altered sphingolipid metabolism with an accumulation of undigested glycosphingolipids in lysosomes due to enzyme deficiency is linked to lysosomal storage disorders, such as Fabry.[36] Build-up of glycosphingolipids in the lysosomes in Fabry disease inhibits lipid recycling, affecting lipid composition of cellular membranes, which results in defects in autophagy flux, mitochondrial, and lysosomal dysfunction.[36]

The low basal levels of cardiac glycosphingolipids we observed are consistent with the low expression of *Ugcg* in heart tissue (Consensus dataset,[25] www.proteinatlas.org (28 June 2021)). During cardiac remodelling, however, cardiac GlcCer levels were elevated in both humans and mice. GlcCer was increased in the septum as well as in the left ventricle, suggesting that this increase is driven by pressure overload or increased uptake of glucose, rather than by the ischaemia/hypoxia *per se*. However, the exact mechanism for the elevation in glycosphingolipids following cardiac remodelling remains to be determined. In addition to the increase in glycosphingolipids in the remodelling heart, the full lipidomics and metabolomics profiles revealed numerous rearrangements in the cardiac composition of lipids, amino acids, and other energy substrates. These results highlight the significance of metabolic regulation of cardiac structure and function.[8]

Membrane lipid composition is important for cellular structure and function, but may be particularly crucial for cardiomyocytes to maintain their contractile function. Constant cycles of contraction and relaxation reshape membrane morphology and thereby affect cardiomechanical signalling.[37] Since glycosphingolipids are membrane lipids, we speculated that cardiac glycosphingolipid levels would increase in response to remodelling. Indeed, mice with cardiomyocyte-specific *Ugcg* deletion (and thus depletion of cardiac glycosphingolipids) developed normally and had normal heart function at baseline, but had markedly reduced contractile capacity under stress and died prematurely from heart failure. These findings show that cardiac glycosphingolipids play an important role in heart physiology and function. Even mice with heterozygous deletion of *Ugcg* had significantly reduced heart function and developed heart failure, indicating that

even small reductions in glycosphingolipids can impair cardiomyocyte function. Our results demonstrating that both elevated cardiac glycosphingolipid levels (as shown in the human remodelling heart with reduced heart function) as well as reduced cardiac glycosphingolipids (as shown in the mouse model) correlate with reduced heart function, may seem contrasting and unpredicted. However, these findings clearly indicate that the preservation of membrane lipids is crucial and highlight the importance of glycosphingolipid homeostasis in cardiomyocyte membranes. It is therefore plausible that a deranged sphingolipid metabolism may contribute to the deterioration of cardiac disease.

Our findings indicate that glycosphingolipid homeostasis is crucial for the cardiomyocyte contractility. Glycosphingolipids, particularly GlcCer, markedly affect the biophysical properties of cellular membranes.[38] Studies of artificial membranes have shown that similarly to ceramide, GlcCer is able to form tightly packed gel domains in membrane bilayers, but displays a higher tendency to promote membrane shape changes.[39] Our results show that a critical level of glycosphingolipids in cardiomyocyte membranes may be particularly important under conditions of cardiac stress and hypertrophy, such as cardiac remodelling. In cardiomyocytes, the membrane connects tightly to the cytoskeleton,[40] indicating that alterations in membrane properties will result in biological actions. In agreement with our findings, it has been suggested that cardiomyocyte hypertrophy during cardiac remodelling is both a means to cope with wall stress and part of a complex feedback system to fine-tune and regulate membrane-mediated signalling.[37]

We found that depletion of glycosphingolipids in cardiomyocytes compromises cellular trafficking by reducing endolysosomal retrograde transport and autophagy. *Ugcg* deficiency reduced the size of LAMP1-positive endolysosomes and reduced Stx5 levels, suggesting defective endosome-to-Golgi transport. Importantly, the Golgi apparatus was dispersed in hearts from young h*Ugcg*$^{-/-}$ mice, even before clear signs of heart failure were present. Our results agree with previous reports showing that glycosphingolipids are essential for functional endocytosis, for example in the intestine[41] and to enable influenza virus entry.[42] Our results also show that *Ugcg*-deficiency results in reduced autophagy through activation of mTORC1, possibly enhancing defects in endolysosomal transport. Indeed, other membrane lipids, such as cholesterol, have been implicated in endolysosomal function and autophagy.[43]

Intact β1AR signalling and trafficking are crucial for cardiac function, and defects in this system contribute to heart failure.[44] Membrane lipid composition is imperative for the function of βARs and other G-protein-coupled receptors,[18,45] and membrane lipids affect the agonist binding, conformation, internalization, and trafficking of several G-protein-coupled receptors.[46–48] We found that β1ARs in *Ugcg*-deficient cardiomyocytes were not internalized after agonist stimulation; most remained at the cell surface, desensitized and unable to transduce receptor signalling. Furthermore, our results show that inhibition of endolysosomal trafficking using EGA results in reduced cAMP production, indicating that the impairment of receptor internalization in glycosphingolipid-depleted cells is due to defective endolysosomal transport between early and late endosomes. Several studies have shown that disturbance of endosomal trafficking can lead to disturbed β-adrenergic signalling and reduced cardiac contraction. Impairments in endocytosis and receptor trafficking lock the β1AR in a desensitized state in the plasma membrane, resulting in a reduced responsiveness to agonist stimulation, reduced contractility, and severe cardiac dysfunction.[49] Inhibition of Rab4 activity, which is involved in the endocytosis of the β2AR, in mouse cardiomyocytes leads to impaired responsiveness to agonist stimulation and heart failure.[50] In addition, knockout of EHD3 (a mediator of endosomal trafficking) blunts the response to βAR stimulation.[51]

Additional work will be necessary to identify the effects of *Ugcg* deficiency beyond those described here. Because autophagy regulates multiple processes that are vital to preserve cardiomyocyte function,[52–54] such as removal of cell debris and damaged organelles,[55] defective autophagy in the heart may have effects in addition to compromised endosomal trafficking.

In conclusion, our study shows that cardiac glycosphingolipids, synthesized through GlcCer synthase, are crucial for maintaining β1AR signalling through the endolysosomal system and that a critical level of glycosphingolipids is necessary to maintain the structure and function of cardiomyocytes and to preserve normal heart function in the long term.

Supplementary material

Supplementary material is available at *European Heart Journal online*.

Acknowledgements

The authors thank Rosie Perkins and Stephen Ordway for editing of the manuscript.

Funding

The Swedish Research Council [2017-01340]; the Swedish Heart and Lung Foundation [20170492]; and the Sahlgrenska University Hospital ALF research grants [ALFGBG-724901].

Conflict of interest: The authors declare that there is no conflict of interest, except for; M.E. reports personal fees from AstraZeneca, outside the submitted work; and A.J. reports personal fees from Boehringer-Ingelheim, Werfen, XVIVO Perfusion, Portola, and LFB, outside the submitted work.

References

1. Braunwald E. Heart failure. *JACC Heart Fail* 2013;**1**:1–20.
2. Burchfield JS, Xie M, Hill JA. Pathological ventricular remodeling: mechanisms: part 1 of 2. *Circulation* 2013;**128**:388–400.
3. Hill JA, Olson EN. Cardiac plasticity. *N Engl J Med* 2008;**358**:1370–1380.
4. Sakamoto T, Kelly DP. A case for adaptive cardiac hypertrophic remodeling is CITED. *Circ Res* 2020;**127**:647–650.
5. Bilheimer DW, Buja LM, Parkey RW, Bonte FJ, Willerson JT. Fatty acid accumulation and abnormal lipid deposition in peripheral and border zones of experimental myocardial infarcts. *J Nucl Med* 1978;**19**:276–283.
6. Drevinge C, Karlsson LO, Stahlman M, Larsson T, Perman Sundelin J, Grip L, Andersson L, Boren J, Levin MC. Cholesteryl esters accumulate in the heart in a porcine model of ischemia and reperfusion. *PLoS One* 2013;**8**:e61942.
7. Klevstig M, Stahlman M, Lundqvist A, Scharin Tang M, Fogelstrand P, Adiels M, Andersson L, Kolesnick R, Jeppsson A, Boren J, Levin MC. Targeting acid sphingomyelinase reduces cardiac ceramide accumulation in the post-ischemic heart. *J Mol Cell Cardiol* 2016;**93**:69–72.
8. Gibb AA, Hill BG. Metabolic coordination of physiological and pathological cardiac remodeling. *Circ Res* 2018;**123**:107–128.
9. Chokshi A, Drosatos K, Cheema FH, Ji R, Khawaja T, Yu S, Kato T, Khan R, Takayama H, Knoll R, Milting H, Chung CS, Jorde U, Naka Y, Mancini DM, Goldberg IJ, Schulze PC. Ventricular assist device implantation corrects myocardial lipotoxicity, reverses insulin resistance, and normalizes cardiac metabolism in patients with advanced heart failure. *Circulation* 2012;**125**:2844–2853.

10. Perman JC, Boström P, Lindbom M, Lidberg U, StÅhlman M, Hägg D, Lindskog H, Scharin Täng M, Omerovic E, Mattsson Hultén L, Jeppsson A, Petursson P, Herlitz J, Olivecrona G, Strickland DK, Ekroos K, Olofsson S-O, Borén J. The VLDL receptor promotes lipotoxicity and increases mortality in mice following an acute myocardial infarction. *J Clin Invest* 2011;**121**:2625–2640.
11. Hicks AA, Pramstaller PP, Johansson A, Vitart V, Rudan I, Ugocsai P, Aulchenko Y, Franklin CS, Liebisch G, Erdmann J, Jonasson I, Zorkoltseva IV, Pattaro C, Hayward C, Isaacs A, Hengstenberg C, Campbell S, Gnewuch C, Janssens AC, Kirichenko AV, Konig IR, Marroni F, Polasek O, Demirkan A, Kolcic I, Schwienbacher C, Igl W, Biloglav Z, Witteman JC, Pichler I, Zaboli G, Axenovich TI, Peters A, Schreiber S, Wichmann HE, Schunkert H, Hastie N, Oostra BA, Wild SH, Meitinger T, Gyllensten U, van Duijn CM, Wilson JF, Wright A, Schmitz G, Campbell H. Genetic determinants of circulating sphingolipid concentrations in European populations. *PLoS Genet* 2009;**5**:e1000672.
12. Akhtar MM, Elliott PM. Anderson-Fabry disease in heart failure. *Biophys Rev* 2018;**10**:1107–1119.
13. Kör Y, Keskin M, Başpınar O. Severe cardiac involvement in Gaucher type IIIC: a case report and review of the literature. *Cardiol Young* 2017;**27**:1426–1429.
14. Ji R, Akashi H, Drosatos K, Liao X, Jiang H, Kennel PJ, Brunjes DL, Castillero E, Zhang X, Deng LY, Homma S, George IJ, Takayama H, Naka Y, Goldberg IJ, Schulze PC. Increased de novo ceramide synthesis and accumulation in failing myocardium. *JCI Insight* 2017;**2**:e96203.
15. Reforgiato MR, Milano G, Fabrias G, Casas J, Gasco P, Paroni R, Samaja M, Ghidoni R, Caretti A, Signorelli P. Inhibition of ceramide de novo synthesis as a postischemic strategy to reduce myocardial reperfusion injury. *Basic Res Cardiol* 2016;**111**:12.
16. Hadas Y, Vincek AS, Youssef E, Żak MM, Chepurko E, Sultana N, Sharkar MTK, Guo N, Komargodski R, Kurian AA, Kaur K, Magadum A, Fargnoli A, Katz MG, Hossain N, Kenigsberg E, Dubois NC, Schadt E, Hajjar R, Eliyahu E, Zangi L. Altering sphingolipid metabolism attenuates cell death and inflammatory response after myocardial infarction. *Circulation* 2020;**141**:916–930.
17. Gault CR, Obeid LM, Hannun YA. An overview of sphingolipid metabolism: from synthesis to breakdown. *Adv Exp Med Biol* 2010;**688**:1–23.
18. Russo D, Parashuraman S, D'Angelo G. Glycosphingolipid-protein interaction in signal transduction. *Int J Mol Sci* 2016;**17**:1732.
19. Sonnino S, Prinetti A. Sphingolipids and membrane environments for caveolin. *FEBS Lett* 2009;**583**:597–606.
20. Futerman AH, Hannun YA. The complex life of simple sphingolipids. *EMBO Rep* 2004;**5**:777–782.
21. Batta G, Soltész L, Kovács T, Bozó T, Mészár Z, Kellermayer M, Szöllősi J, Nagy P. Alterations in the properties of the cell membrane due to glycosphingolipid accumulation in a model of Gaucher disease. *Sci Rep* 2018;**8**:157.
22. D'Angelo G, Capasso S, Sticco L, Russo D. Glycosphingolipids: synthesis and functions. *FEBS J* 2013;**280**:6338–6353.
23. Russo D, Capolupo L, Loomba JS, Sticco L, D'Angelo G. Glycosphingolipid metabolism in cell fate specification. *J Cell Sci* 2018;**131**:jcs219204.
24. Yamashita T, Allende ML, Kalkofen DN, Werth N, Sandhoff K, Proia RL. Conditional LoxP-flanked glucosylceramide synthase allele controlling glycosphingolipid synthesis. *Genesis* 2005;**43**:175–180.
25. Uhlén M, Fagerberg L, Hallström BM, Lindskog C, Oksvold P, Mardinoglu A, Sivertsson Å, Kampf C, Sjöstedt E, Asplund A, Olsson I, Edlund K, Lundberg E, Navani S, Szigyarto CA-K, Odeberg J, Djureinovic D, Takanen JO, Hober S, Alm T, Edqvist P-H, Berling H, Tegel H, Mulder J, Rockberg J, Nilsson P, Schwenk JM, Hamsten M, von Feilitzen K, Forsberg M, Persson L, Johansson F, Zwahlen M, von Heijne G, Nielsen J, Pontén F. Proteomics. Tissue-based map of the human proteome. *Science* 2015;**347**:1260419.
26. Tai G, Lu L, Wang TL, Tang BL, Goud B, Johannes L, Hong W. Participation of the syntaxin 5/Ykt6/GS28/GS15 SNARE complex in transport from the early/recycling endosome to the trans-Golgi network. *Mol Biol Cell* 2004;**15**:4011–4022.
27. Rabouille C, Kondo H, Newman R, Hui N, Freemont P, Warren G. Syntaxin 5 is a common component of the NSF- and p97-mediated reassembly pathways of Golgi cisternae from mitotic Golgi fragments in vitro. *Cell* 1998;**92**:603–610.
28. Mauthe M, Orhon I, Rocchi C, Zhou X, Luhr M, Hijlkema KJ, Coppes RP, Engedal N, Mari M, Reggiori F. Chloroquine inhibits autophagic flux by decreasing autophagosome-lysosome fusion. *Autophagy* 2018;**14**:1435–1455.
29. Hwang JY, Gertner M, Pontarelli F, Court-Vazquez B, Bennett MV, Ofengeim D, Zukin RS. Global ischemia induces lysosomal-mediated degradation of mTOR and activation of autophagy in hippocampal neurons destined to die. *Cell Death Differ* 2017;**24**:317–329.
30. Brown RA, Voit A, Srikanth MP, Thayer JA, Kingsbury TJ, Jacobson MA, Lipinski MM, Feldman RA, Awad O. mTOR hyperactivity mediates lysosomal dysfunction in Gaucher's disease iPSC-neuronal cells. *Dis Model Mech* 2019;**12**:dmm038596.
31. Tang Y, Hu LA, Miller WE, Ringstad N, Hall RA, Pitcher JA, DeCamilli P, Lefkowitz RJ. Identification of the endophilins (SH3p4/p8/p13) as novel binding partners for the beta1-adrenergic receptor. *Proc Natl Acad Sci U S A* 1999;**96**:12559–12564.
32. Hakalahti AE, Khan H, Vierimaa MM, Pekkala EH, Lackman JJ, Ulvila J, Kerkela R, Petaja-Repo UE. Beta-adrenergic agonists mediate enhancement of beta1-adrenergic receptor N-terminal cleavage and stabilization in vivo and in vitro. *Mol Pharmacol* 2013;**83**:129–141.
33. Nooh MM, Chumpia MM, Hamilton TB, Bahouth SW. Sorting of beta1-adrenergic receptors is mediated by pathways that are either dependent on or independent of type I PDZ, protein kinase A (PKA), and SAP97. *J Biol Chem* 2014;**289**:2277–2294.
34. Hall RA, Premont RT, Chow CW, Blitzer JT, Pitcher JA, Claing A, Stoffel RH, Barak LS, Shenolikar S, Weinman EJ, Grinstein S, Lefkowitz RJ. The beta2-adrenergic receptor interacts with the Na+/H+-exchanger regulatory factor to control Na+/H+ exchange. *Nature* 1998;**392**:626–630.
35. Hanyaloglu AC, von Zastrow M. Regulation of GPCRs by endocytic membrane trafficking and its potential implications. *Annu Rev Pharmacol Toxicol* 2008;**48**:537–568.
36. Ivanova M. Altered sphingolipids metabolism damaged mitochondrial functions: lessons learned from Gaucher and Fabry diseases. *J Clin Med* 2020;**9**:1116.
37. Knoll R. A role for membrane shape and information processing in cardiac physiology. *Pflugers Arch* 2015;**467**:167–173.
38. Varela AR, Ventura AE, Carreira AC, Fedorov A, Futerman AH, Prieto M, Silva LC. Pathological levels of glucosylceramide change the biophysical properties of artificial and cell membranes. *Phys Chem Chem Phys* 2016;**19**:340–346.
39. Varela AR, Goncalves da Silva AM, Fedorov A, Futerman AH, Prieto M, Silva LC. Effect of glucosylceramide on the biophysical properties of fluid membranes. *Biochim Biophys Acta* 2013;**1828**:1122–1130.
40. Samarel AM. Focal adhesion signaling in heart failure. *Pflugers Arch* 2014;**466**:1101–1111.
41. Jennemann R, Kaden S, Sandhoff R, Nordstrom V, Wang S, Volz M, Robine S, Amen N, Rothermel U, Wiegandt H, Grone HJ. Glycosphingolipids are essential for intestinal endocytic function. *J Biol Chem* 2012;**287**:32598–32616.
42. Drews K, Calgi MP, Harrison WC, Drews CM, Costa-Pinheiro P, Shaw JJP, Jobe KA, Han JD, Fox TE, White JM, Kester M. Glucosylceramide synthase maintains influenza virus entry and infection. *PLoS One* 2020;**15**:e0228735.
43. Wijdeven RH, Janssen H, Nahidiazar L, Janssen L, Jalink K, Berlin I, Neefjes J. Cholesterol and ORP1L-mediated ER contact sites control autophagosome transport and fusion with the endocytic pathway. *Nat Commun* 2016;**7**:11808.
44. Lefkowitz RJ, Rockman HA, Koch WJ. Catecholamines, cardiac beta-adrenergic receptors, and heart failure. *Circulation* 2000;**101**:1634–1637.
45. Jafurulla M, Chattopadhyay A. Sphingolipids in the function of G protein-coupled receptors. *Eur J Pharmacol* 2015;**763**:241–246.
46. Harikumar KG, Puri V, Singh RD, Hanada K, Pagano RE, Miller LJ. Differential effects of modification of membrane cholesterol and sphingolipids on the conformation, function, and trafficking of the G protein-coupled cholecystokinin receptor. *J Biol Chem* 2005;**280**:2176–2185.
47. Sjogren B, Svenningsson P. Depletion of the lipid raft constituents, sphingomyelin and ganglioside, decreases serotonin binding at human 5-HT7(a) receptors in HeLa cells. *Acta Physiol (Oxf)* 2007;**190**:47–53.
48. Manna M, Niemela M, Tynkkynen J, Javanainen M, Kulig W, Muller DJ, Rog T, Vattulainen I. Mechanism of allosteric regulation of beta2-adrenergic receptor by cholesterol. *Elife* 2016;**5**:e18432.
49. Jean-Charles PY, Yu SM, Abraham D, Kommaddi RP, Mao L, Strachan RT, Zhang ZS, Bowles DE, Brian L, Stiber JA, Jones SN, Koch WJ, Rockman HA, Shenoy SK. Mdm2 regulates cardiac contractility by inhibiting GRK2-mediated desensitization of beta-adrenergic receptor signaling. *JCI Insight* 2017;**2**:e95998.
50. Odley A, Hahn HS, Lynch RA, Marreez Y, Osinska H, Robbins J, Dorn GW 2nd. Regulation of cardiac contractility by Rab4-modulated beta2-adrenergic receptor recycling. *Proc Natl Acad Sci U S A* 2004;**101**:7082–7087.
51. Curran J, Makara MA, Little SC, Musa H, Liu B, Wu X, Polina I, Alecusan JS, Wright P, Li J, Billman GE, Boyden PA, Gyorke S, Band H, Hund TJ, Mohler PJ. EHD3-dependent endosome pathway regulates cardiac membrane excitability and physiology. *Circ Res* 2014;**115**:68–78.
52. Kim YC, Park HW, Sciarretta S, Mo JS, Jewell JL, Russell RC, Wu X, Sadoshima J, Guan KL. Rag GTPases are cardioprotective by regulating lysosomal function. *Nat Commun* 2014;**5**:4241.
53. Nakai A, Yamaguchi O, Takeda T, Higuchi Y, Hikoso S, Taniike M, Omiya S, Mizote I, Matsumura Y, Asahi M, Nishida K, Hori M, Mizushima N, Otsu K. The role of autophagy in cardiomyocytes in the basal state and in response to hemodynamic stress. *Nat Med* 2007;**13**:619–624.
54. Sciarretta S, Maejima Y, Zablocki D, Sadoshima J. The role of autophagy in the heart. *Annu Rev Physiol* 2018;**80**:1–26.
55. Woodall BP, Gustafsson AB. Autophagy-A key pathway for cardiac health and longevity. *Acta Physiol (Oxf)* 2018;**223**:e13074.